Molecular Ecology 28 (2019) : 3257-3270 DOI: 10.1111/mec.15133

Phylogeography of a cryptic speciation continuum in Eurasian spadefoot toads (*Pelobates*)

Christophe Dufresnes[1,2,3], Ilias Strachinis[4], Nataliia Suriadna[5], Galyna Mykytynets[6], Dan Cogălniceanu[7], Paul Székely[8], Tanja Vukov[9], Jan W Arntzen[10], Ben Wielstra[10,11], Petros Lymberakis[12], Eli Geffen[13], Sarig Gafny[14], Yusuf Kumlutaş[15,16], Çetin Ilgaz[15,16], Kamil Candan[15,16], Edvard Mizsei[17], Márton Szabolcs[17], Krzysztof Kolenda[18], Nazar Smirnov[19], Philippe Géniez[20], Simeon Lukanov[21], Pierre-André Crochet[22], Sylvain Dubey[2, 23, 24], Nicolas Perrin[23], Spartak N Litvinchuk[25,26,*], Mathieu Denoël[27,*]

[1]*Department of Animal and Plant Sciences, University of Sheffield, Sheffield, UK*
[2]*Hintermann & Weber SA, Montreux, Switzerland*
[3]*Laboratory for Conservation Biology, University of Lausanne, Lausanne, Switzerland*
[4]*School of Biology, Aristotle University of Thessaloniki, Thessaloniki, Greece*
[5]*Melitopol Insitute of Ecology and Social Technologies of University "Ukraine", Melitopol, Zaporizhia, Ukraine*
[6]*Pryazovsky National Nature Park, Melitopol, Zaporizhia, Ukraine*
[7]*Faculty of Natural Sciences and Agricultural Sciences, University Ovidius Constanţa, Constanţa, Romania*
[8]*Departamento de Ciencias Biológicas, EcoSs Lab, Universidad Técnica Particular de Loja, Loja, Ecuador*
[9]*Department of Evolutionary Biology, Institute for Biological Research "Siniša Stanković", National Institute of Republic of Serbia, University of Belgrade, Belgrade, Serbia*
[10]*Naturalis Biodiversity Center, Leiden, The Netherlands*
[11]*Institute of Biology Leiden, Leiden University, Leiden, The Netherlands*
[12]*Natural History Museum of Crete, University of Crete, Irakleio, Crete, Greece*
[13]*School of Zoology, Tel Aviv University, Tel Aviv, Israel*
[14]*School of Marine Sciences, Ruppin Academic Center, Michmoret, Israel*
[15]*Department of Biology, Faculty of Science, Dokuz Eylül University, Buca, İzmir, Turkey*
[16]*Research and Application Center for Fauna and Flora, Dokuz Eylül University, Buca, İzmir, Turkey*
[17]*Department of Tisza River Research, Danube Research Institute, Centre for Ecological Research, Hungarian Academy of Sciences, Debrecen, Hungary*
[18]*Department of Evolutionary Biology and Conservation of Vertebrates, Institute of Environmental Biology, University of Wrocław, Wrocław, Poland*
[19]*Department of Nature, Chernivtsi Regional Museum, Chernivtsi, Ukraine*
[20]*CEFE, EPHE-PSL, CNRS, University of Montpellier, University Paul Valéry Montpellier 3, IRD, Montpellier, France*
[21]*Institute of Biodiversity and Ecosystem Research, Bulgarian Academy of Sciences, Sofia, Bulgaria*
[22]*CEFE, CNRS, University of Montpellier, University Paul Valéry Montpellier 3, EPHE, IRD, Montpellier, France*
[23]*Department of Ecology and Evolution, University of Lausanne, Lausanne, Switzerland*
[24]*Agrosustain SA, Nyon, Switzerland*
[25]*Institute of Cytology, Russian Academy of Sciences, St. Petersburg, Russia*
[26]*Department of Zoology and Physiology, Dagestan State University, Makhachkala, Russia*
[27]*Laboratory of Fish and Amphibian Ethology, Behavioural Biology Group, Freshwater and OCeanic science Unit of reSearch (FOCUS), University of Liège, Liège, Belgium*

*Spartak N. Litvinchuk and Mathieu Denoël have contributed equally

Abstract

Cryptic phylogeographic diversifications provide unique models to examine the role of phylogenetic divergence on the evolution of reproductive isolation, without extrinsic factors such as ecological and behavioural differentiation. Yet, to date very few comparative studies have been attempted within such radiations. Here, we characterize a new speciation continuum in a group of widespread Eurasian amphibians, the *Pelobates* spadefoot toads, by conducting multilocus (restriction site associated DNA sequencing and mitochondrial DNA) phylogenetic, phylogeographic and hybrid zone analyses. Within the *P. syriacus* complex, we discovered species-level cryptic divergences (>5 million years ago [My]) between populations distributed in the Near-East (hereafter *P. syriacus sensu stricto* [*s.s.*]) and southeastern Europe (hereafter *P. balcanicus*), each featuring deep intraspecific lineages. Altogether, we could scale hybridizability to divergence time along six different stages, spanning from sympatry without gene flow (*P. fuscus* and *P. balcanicus*, >10 My), parapatry with highly restricted hybridization (*P. balcanicus* and *P. syriacus s.s.*, >5 My), narrow hybrid zones (~15 km) consistent with partial reproductive isolation (*P. fuscus* and *P. vespertinus*, ~3 My), to extensive admixture between Pleistocene and refugial lineages (≤2 My). This full spectrum empirically supports a gradual build up of reproductive barriers through time, reversible up until a threshold that we estimate at ~3 My. Hence, cryptic phylogeographic lineages may fade away or become reproductively isolated species simply depending on the time they persist in allopatry, and without definite ecomorphological divergence.

1 INTRODUCTION

The cryptic diversifications frequently discovered within traditionally described taxa are hallmarks of the continuum from population divergence to speciation (Avise, 2000; Avise, Walker, & Johns, 1998; Bickford et al., 2006). Disentangling between shallow, ephemeral divergences (e.g., refugial lineages) versus deep, evolutionary significant units, and testing for their reproductive isolation across natural hybrid zones are major issues in molecular ecology. These are the initial steps to delimit cryptic taxa in an integrative manner (Padial, Miralles, De la Riva, & Vences, 2010), which can provide insights into the mechanisms and timeframes creating and maintaining diversity within species complexes.

Because speciation is often a multidimensional process involving a combination of genetic, geographical, behavioural and ecological factors (Mérot, Salazar, Merrill, Jiggins, & Joron, 2017; Nosil, Feder, Flaxman, & Gompert, 2017), predicting the evolutionary fate of nascent lineages comes close to a wild guess. An alternative is to focus on single radiations consisting of ecologically and morphologically similar lineages that are meeting in secondary contact zones. Such systems offer “natural laboratories” to gauge how reproductive isolation evolves along the speciation continuum under comparable contexts of life history and genetic backgrounds. The modality of the relationship between hybridizability and divergence time should thus be only bounded by the genetic architecture of Dobzhansky–Muller incompatibilities (DMIs) and the interactions between demographic (drift and dispersal) and

selective forces (pre- and post-zygotic isolation) (Gavrilets, 2004; Gourbiere & Mallet, 2009; Orr, 1995). It should be gradual if DMIs build up progressively with genetic divergence. Theoretical (Gourbiere & Mallet, 2009) and empirical work (Mendelson, Inouye, & Rausher, 2004; Singhal & Moritz, 2013) posit an exponential increase through time if incompatibilities cumulate multiplicatively (not additively) as barriers to gene flow start to evolve. Speciation can thus be viewed as an accelerating process, irreversibly isolating nascent species once a threshold of genetic divergence has been reached (Roux et al., 2016). From an applied perspective, the timeframe of speciation can serve as an ad hoc metric to assist taxonomic decisions of ambiguous phylogeographic splits, particularly for allopatric lineages that do not naturally meet in the wild.

Nevertheless, so far only a handful of cryptic radiations have been comprehensively investigated under natural settings, including enough species pairs for comparative assessments. These have yielded contrasting outcomes. The link between reproductive isolation and genetic differentiation ranged from unequivocal in Australian rainforest skinks (Singhal & Moritz, 2013), weak in *Triturus* newts (Arntzen, Wielstra, & Wallis, 2014), to seemingly absent in the tree weta *Hemideina thoracia* (Morgan-Richards & Wallis, 2003). A qualitative trend is palpable in other systems (e.g., Pabijan, Zielinski, Dudek, Stuglik, & Babik, 2017), although often with strong variation between replicate contacts (Dufresnes et al., 2018 and references therein). Accordingly, the correlation between divergence time and reproductive isolation can easily be blurred by the heterogeneity of local hybrid zone dynamics. Demographic and landscape factors, such as opportunities for dispersal and biogeographic history are also major determinants of hybrid zone structure (Barton & Hewitt, 1985; Beysard & Heckel, 2014; Smadja & Butlin, 2011). For the same species pairs, this can for instance lead to drastically different levels of admixture depending on the time since their initial contact (e.g., Croucher, Jones, Searle, & Oxford, 2007). Previous investigations were also remarkably heterogeneous in their molecular resources, such as diagnostic single nucleotide polymorphisms (SNPs) genotyped by enzyme restriction (Singhal & Moritz, 2013), microsatellites (Beysard & Heckel, 2014), allozymes (Arntzen et al., 2014) and cytogenetic differentiation (Morgan-Richards & Wallis, 2003). Against this background of disparities, comparative data from additional cryptic radiations are thus needed to scale hybridizability with divergence time, and get a more comprehensive overview of the modality of the buildup of reproductive isolation under allopatric regimes. Such inferences can now benefit from population genomic tools (e.g., restriction site associated DNA-sequencing [RAD-seq]), which offer a genome-wide resolution to examine the interactions between closely related phylogeographic lineages (Coates, Byrne, & Moritz, 2018).

Eurasian spadefoot toads (*Pelobates*, Pelobatidae) make an attractive yet underexploited system to study the relationships between lineages speciating *in statu nascendi*. In particular, the taxa inhabiting eastern ranges potentially represent multiple stages along the speciation continuum. First, the distribution of the morphologically differentiated *P. syriacus* (Balkans and Asia Minor) and *P. fuscus* (Northern Europe) slightly overlap in the Caucasus and in the Balkans, where they are sympatric and even syntopic (Iosif, Papes, Samoila, & Cogălniceanu, 2014), suggesting complete reproductive isolation. Second, the European *P. fuscus* consists of

independent Balkan (*fuscus*) and Black Sea (*vespertinus*) ecomorphologically similar lineages of Plio-Pleistocene origin that now meet in the Eastern European plains (Borkin et al., 2003; Crottini et al., 2007; Litvinchuk et al., 2013; Suriadna, Mikitinets, Rozanov, Yu, & Litvinchuk, 2016) and hybridize along a narrow transition zone (Litvinchuk et al., 2013). Third, *P. syriacus* features cryptic Asian (*P. s. syriacus*) and European (*P. s. balcanicus*) subspecies, supported by divergent mitochondrial and nuclear haplotypes, as well as allozyme variation, perhaps as old as the Pliocene (Ehl, Vences, & Veith, 2019; Litvinchuk et al., 2013; Veith, Fromhage, Kosuch, & Vences, 2006). So far, no phylogeographic work has focused on *P. syriacus*, and its diversity, distribution and the potential reproductive isolation between lineages remain unknown. Many Eastern Mediterranean amphibians feature species-level divergence between continental Europe and Turkey, forming secondary contact zones in northwestern Anatolia or in the Balkans (e.g., Stöck et al., 2012; Pabijan et al., 2017; Wielstra et al., 2017; Wielstra, Burke, Butlin, & Arntzen, 2017). Moreover, Anatolia, the Levantine region (Eastern Mediterranean coast), the Hyrcanian region (Southern Caspian coast), as well as the Caucasus are important hotspots of diversity (Myers, Mittermeier, Mittermeier, Da Fonseca, & Kent, 2000), at both the interspecific and the intraspecific levels. Therefore, *P. syriacus* could consist of cryptic evolutionary lineages that potentially represent speciation events.

In this study, we present comprehensive molecular investigations of *Pelobates*, combining mitochondrial DNA (mtDNA) phylogenetics, nuclear phylogenomics and population genomics of RAD-seq loci, with a special focus on the phylogeography of *P. syriacus* and the contact zones between parapatric and sympatric lineages in Eastern Europe and the Near-East. We first test whether *P. syriacus* has cryptically diversified across its range, as expected under biogeographic paradigms for the Eastern Mediterranean region. We then characterize the speciation continuum of *Pelobates* through comparative hybrid zone analyses. If reproductive isolation progressively builds up with genetic isolation, we predict that, as divergence time increases, the geographic transitions between two lineages should become narrower and admixed individuals should exhibit less introgression.

2 METHODS

On a nomenclatural note, our present findings led to taxonomic revisions for *Pelobates syriacus*, hereafter referred to *P. syriacus sensu lato* (*s.l.*), as it corresponds to four different taxa: *P. syriacus syriacus* in the Levant, *P. s. boettgeri* in the Caucasus and Anatolia, *P. balcanicus balcanicus* in the Balkans and *P. b. chloeae* in the Peloponnese. We also provide decisive evidence that the *fuscus* and *vespertinus* lineages correspond to distinct species, hereafter noted *P. fuscus* and *P. vespertinus*. The new taxonomy and names are detailed in an accompanying publication (Dufresnes, Strachinis, Tzoras, Litvinchuk, & Denoël, 2019), and are implemented hereafter for clarity. The present paper is not issued for purposes of zoological nomenclature and is thus not published under the meaning of the International Code of Zoological Nomenclature (Art. 8.2). New names that it contains are therefore not made available in the present work.

2.1 DNA sampling

Tissues were collected from wild-caught adults (buccal swabs and toe clips), road kills, tadpoles (tail tips) and museum specimens (skin and muscle pieces) from the following herpetological collections: NHMC (Natural History Museum of Crete), ZMMSU (Zoological Museum of Moscow State University), ZNKSU (Zoological Museum of Kharkov State University), ZISP (Zoological Institute of St Petersburg), IBISS (Institute for Biological Research "Siniša Stanković") and BEV (CEFE – EPHE collection of the Biogeography and Ecology of the Vertebrates team in Montpellier). Samples were preserved at −20°C (buccal swabs) or 70%–100% ethanol (other samples), and extracted with the Qiagen Biosprint Robotic Workstation. A total of 403 individuals were analysed: 253 from *P. syriacus s.l.*, 115 from the contact zone between the *fuscus* and *vespertinus* lineages in southern Ukraine and Western Russia, 16 from Central European *P. fuscus* (including five syntopic with *P. syriacus s.l.*), three from pure *P. vespertinus*, 11 *P. cultripes* and five *P. varaldii* (Table S1). An additional four samples of North American Scaphiopodids (one *Spea bombifrons* and three *Scaphiopus couchii*), close relatives of Pelobatids, were included as outgroups (Table S1). Live animals were sampled for DNA under collecting permits issued by the Israeli Nature and Parks Authority (INPA; 28407/2006–2008), the Greek Ministry of Environment & Energy (ADA: ΩΣΜ34653Π8-9ΣΟ, protocol number: 176158/2249), the Danube Delta Biosphere Reserve Administration and the Ministry of the Environment of Romania (M.O. 1173/27.08.2010), the Polish General Directorate of Environmental Protection (WZP-WG.6401.02.4.2017.dł) and the Bulgarian Ministry of Environment and Water (permit 656/08.12.2015).

2.2 mtDNA genotyping

A total of 107 samples from the *P. fuscus*/*vespertinus* contact zone was DNA-barcoded by sequencing a short fragment (~460 bp) of the mitochondrial *cytochrome-b* (*cyt-b*) with custom primers Pb-cytb-F1: (5′-TACATCGGAAACGTACTAGT-3′) and Pb-cytb-R2 (5′-TTRGCRATWAGGGATCAGAATAG-3′). In other parts of the range, 69 samples were first mitotyped with these primers. For more detailed phylogeographic and phylogenetic analyses, we then sequenced a larger *cyt-b* fragment (~700 bp, primers Pb-cytb-F1 and H15915-short2: 5′-TCATCTCCGGTTTACAAGAC-3′), and ~650 bp of the 16S gene (primers 16SA: 5′-CGCCTGTTTATCAAAAACAT-3′ and 16SB: 5′-CCCGTCTGAACTCAGATCACG-3′) in 265 and 272 individuals, respectively (Table S1).

All polymerase chain reactions (PCRs) were carried out in 25-µl reactions containing 3 µl of template DNA, 12.5 µl of nanopure water, 7.5 µl of multiplex master mix (Qiagen, containing buffer, dNTPs and hot-start polymerase) and 1 µl of each primer (10 µl). PCRs were run as follows: 95°C for 15 min, 35 cycles of 94°C for 30 s, 53°C for 45 s and 72°C for 1 min; and 72°C for 5 min. Sanger sequencing was performed in one direction with primers Pb-cytb-F1, H15915-short2 and 16SA, respectively, for each of the three fragments.

2.3 RAD-sequencing

We prepared three libraries following the double digest RAD (ddRAD) protocol detailed in Brelsford, Dufresnes, and Perrin (2016). Library 1 featured 81 samples selected to study the phylogeny of *Pelobates* and the phylogeography of *P. syriacus s.l.* (Table S1), as well as the four outgroup samples, and was sequenced by two lanes on an Illumina Hi-Seq 2,500 (single read 125). Libraries 2 and 3 focused on the contact zone between *P. fuscus* and *P. vespertinus*, and respectively included 48 (loc. FV1-5 in South Ukraine; Table S1) and 60 samples (loc. FV6-28 in North Ukraine and West Russia; Table S1), and were sequenced on one Illumina lane each (single read 125). After a quality-check (fastqc version 0.10.1), the raw sequences were processed with stacks version 1.48 (Catchen, Hohenlohe, Bassham, Amores, & Cresko, 2013), including demultiplexing (*process_radtags*), stacking and cataloguing of homologous loci (*ustacks*, *cstacks* and *sstacks*) using default *-m -n*, and *-M* values. SNPs were called by *populations* with filters on minor allele frequency (*-min_maf* of 0.05) and maximum observed heterozygosity (*-max_obs_het* of 0.75) to account for over-merging of paralogous loci. We outputted several sequence alignments and SNP matrices from different subsets of samples, calling only loci present in all of them. This allowed us to optimize the amount of data for each analysis. The outgroup samples were uninformative, as they did not share RAD tags with the Palearctic *Pelobates*.

2.4 Phylogenetic and demographic analyses

We performed Bayesian phylogenetic reconstructions of the mtDNA and nuclear data. For mtDNA, this involved 60 unique 1,198 bp haplotypes concatenated from 16S (541 bp) + *cyt-b* (657 bp), identified from 256 *Pelobates* individuals for which both genes were successfully sequenced (Table S1). Three mitochondrial GenBank sequences from *Spea bombifrons* (JX564896), *Scaphiopus couchii* (JX564894) and *Scaphiopus holbrookii* (NC037377) were used as outgroups. The nuclear data consisted of an unpartitioned 63.5 kb alignment concatenating 538 RAD tags from 53 individuals representing all *Pelobates* lineages identified, including 37 toads from seemingly pure populations of the different *P. syriacus s.l.* nuclear clusters (Table S1, see Results). In the absence of outgroup sequences (see above), we midpoint-rooted the nuclear tree by the common ancestor of the *P. cultripes*/*P. varaldii* clade and the rest of *Pelobates*. Indeed, the branch leading to the *P. cultripes*/*P. varaldii* clade is the most basal one (Crottini et al., 2007).

Phylogenetic analyses were conducted with beast 2.4.8 (module starBEAST, Bouckaert et al., 2014). We used a lognormal relaxed molecular clock calibrated to the split between the Iberian *P. cultripes* and Moroccan *P. varaldii* at the end of the Messinian Salinity Crisis (MSC; 5.33 ± 1.0 million years ago, Crottini et al., 2007) with a normally distributed prior and a birth–death tree model. Substitution models were selected with the beast package bModelTest (Bouckaert & Drummond, 2017): HKY + G, GTR and GTR + G for *cyt-b*, 16S and nuclear data, respectively. Chains were run for 100 million iterations, sampling one tree every 50,000. We verified stationarity and effective sample sizes of parameters with tracer 1.5, and built maximum-clade credibility trees with the beast module TreeAnnotator, discarding the first 20%

of sampled trees as burnin. We also visualized all sampled trees with densitree 2.2.6 (Bouckaert & Heled, 2014). Furthermore, we computed pairwise nucleotide distances as a standard metric of divergence between the main clades.

We inferred the demographic history of the two most widespread *P. syriacus s.l.* lineages, namely populations from the Balkans (loc. 24–64, *P. b. balcanicus*) and from European Turkey/Limnos/Anatolia/Caucasus (loc. 6–23. *P. s. boettgeri*) with the Extended Bayesian Skyline Plot (EBSP, Heled & Drummond, 2008), combining unpartitioned alignments of RAD tags (respectively 1.3 and 1.9 Mb) and partitioned mtDNA alignments (16S + *cyt-b*, 1,198 bp). The analysis was set up following the recommendations of Heled (2015) for beast 2, using the same substitution models as above. Chains were run for 100 million iterations, sampling one tree every 10,000. Final graphs were produced with the custom R script provided by Heled (2010), with a burnin cutoff of 20%. EBSP reconstructions can be sensitive to deep population structure, which can cause artefactual signals of population declines (Stoffel et al., 2015 and references therein). For this reason, we did not include our few samples from the genetically differentiated loc. 1–5 (*P. s. syriacus*), loc. 65 (southern mtDNA lineage of *P. b. balcanicus*) and loc. 66 (*P. b. chloeae*) in the EBSP.

2.5 Population genetics

To visualize the genetic structure among all Palearctic spadefoot toads, we first performed a principal component analysis (PCA) on individual genotypes with the R packages *ade4* and *adegenet* (Jombart, 2008), based on 677 SNPs sequenced in all samples/species of library 1 ($n = 81$). We then computed PCAs separately for the distinct species *P. syriacus s.s*. (loc. 1–23, $n = 25$, 12,665 SNPs) and *P. balcanicus* (loc. 24–66, $n = 40$, 13,146 SNPs).

Nuclear population differentiation within these two species was further inferred with the Bayesian clustering algorithm of structure (Pritchard, Stephens, & Donnelly, 2000). We used the admixture model and ran three replicate runs for $K = 1$ to 6, each consisting of 100,000 iterations after 10,000 of burnin, and computed the ΔK statistics with structure harvester (Earl & vonHoldt, 2012). We also calculated observed heterozygosity (H_O) for each population with the R package *hierfstat*.

2.6 Analyses of *Pelobates* contact zones

We explored genetic admixture between three pairs of taxa of varying levels of divergence (see Results): *P. fuscus* and *P. b. balcanicus*, which are sympatric in the Central Balkans ($n = 186$ and $n = 38$, for mtDNA and 3,411 nuclear SNPs, respectively); *P. b. balcanicus* and *P. s. boettgeri*, which meet in European Turkey ($n = 202$ and $n = 50$ for mtDNA and 10,735 nuclear SNPs, respectively); and *P. fuscus* and *P. vespertinus*, which hybridize in Southern Ukraine ($n = 41$ and $n = 48$ for mtDNA and 23,253 nuclear SNPs, respectively) and Northern Ukraine/Western Russia ($n = 66$ and $n = 60$ for mtDNA and 11,006 nuclear SNPs, respectively).

For each contact zone, we conducted structure analyses with $K = 2$, as described above, and mapped mtDNA and nuclear gene pools. The two different data sets for the *P. fuscus*/*vespertinus* hybrid zones were analysed separately. Finally, we performed cline analysis of a transition between *P. fuscus* and *P. vespertinus* at loc. FV16-24, which corresponds to a continuous east–west transect of a local contact along the Psel River in Kursk Oblast, Russia. Sigmoid clines were fitted to mtDNA allele frequency data and nuclear hybrid index (structure ancestry coefficient) along this transect, with the R package *hzar* (Derryberry, Derryberry, Maley, & Brumfield, 2014). Model selection was performed between the different cline models with or without exponential tails.

3 RESULTS

3.1 Genetic relationships of *Pelobates* spadefoot toads

Mitochondrial (*cyt-b* + 16S, 1.2 kb) and nuclear (538 RAD tags, 63.5 kb) phylogenies revealed that *Pelobates syriacus s.l.* represents two distinct clades of Mio-Pliocene divergence: *P. balcanicus* in Europe and *P. syriacus s.s.* in the Near East (Figure 1). Both clades feature subclades of Pleistocene divergences (Table 1), namely *P. b. balcanicus* (Balkans; blue) and *P. b. chloeae* (Peloponnese; purple), and *P. s. syriacus* (Levant; orange) and *P. s. boettgeri* (Caucasus, Anatolia, European Turkey and Limnos; yellow). The European *P. b. balcanicus* diversified into shallow nuclear and mitochondrial lineages in the eastern (E-Romania, E-Bulgaria, NE-Greece; medium blue) and the western parts (NW-Greece, Albania, Northern Macedonia, Serbia, W-Romania, SW-Bulgaria; cyan) of the Balkan Peninsula, and we report a third mtDNA subclade on the coastal island of Evia in S-Greece (dark blue). The phylogenies also confirmed the divergence of *P. fuscus* (dark green) and *P. vespertinus* (light green) since the late Pliocene/early Pleistocene, as well as between the Iberian (*P. cultripes*; grey) and Moroccan species (*P. varaldii*; black), that we used as calibration. Several internal nodes were not resolved, namely the respective positions of *P. balcanicus*, *P. syriacus* and *P. fuscus*/*vespertinus* (Figure S1). Accordingly, confidence intervals for the ages of these nodes were large (Figure 1).

Table 1. Mitochondrial and nuclear divergence time estimates (medians; million years ago) for the interacting pairs of *Pelobates* lineages, and description of the contact

Pair of lineages	mtDNA	Nuclear	Contact zone
P. fuscus versus *P. balcanicus*	12.4	12.6	Sympatry without admixture
P. balcanicus versus *P. syriacus*	10.5	6.6	Parapatry with highly-restricted admixture
P. fuscus versus *P. vespertinus*	2.2	3.2	Parapatry with restricted admixture (~15 km)
P. b. balcanicus versus *P. b. chloeae*	2.2	1.8	Admixture in northern Greece
P. s. syriacus versus *P. s. boettgeri*	1.1	1.4	Admixture across Caucasus/Anatolia/Levant
P. b. balcanicus W versus E	0.4	0.9	Admixture over the entire Balkan Peninsula
P. b. balcanicus S versus E/W	0.5	–	No assessment

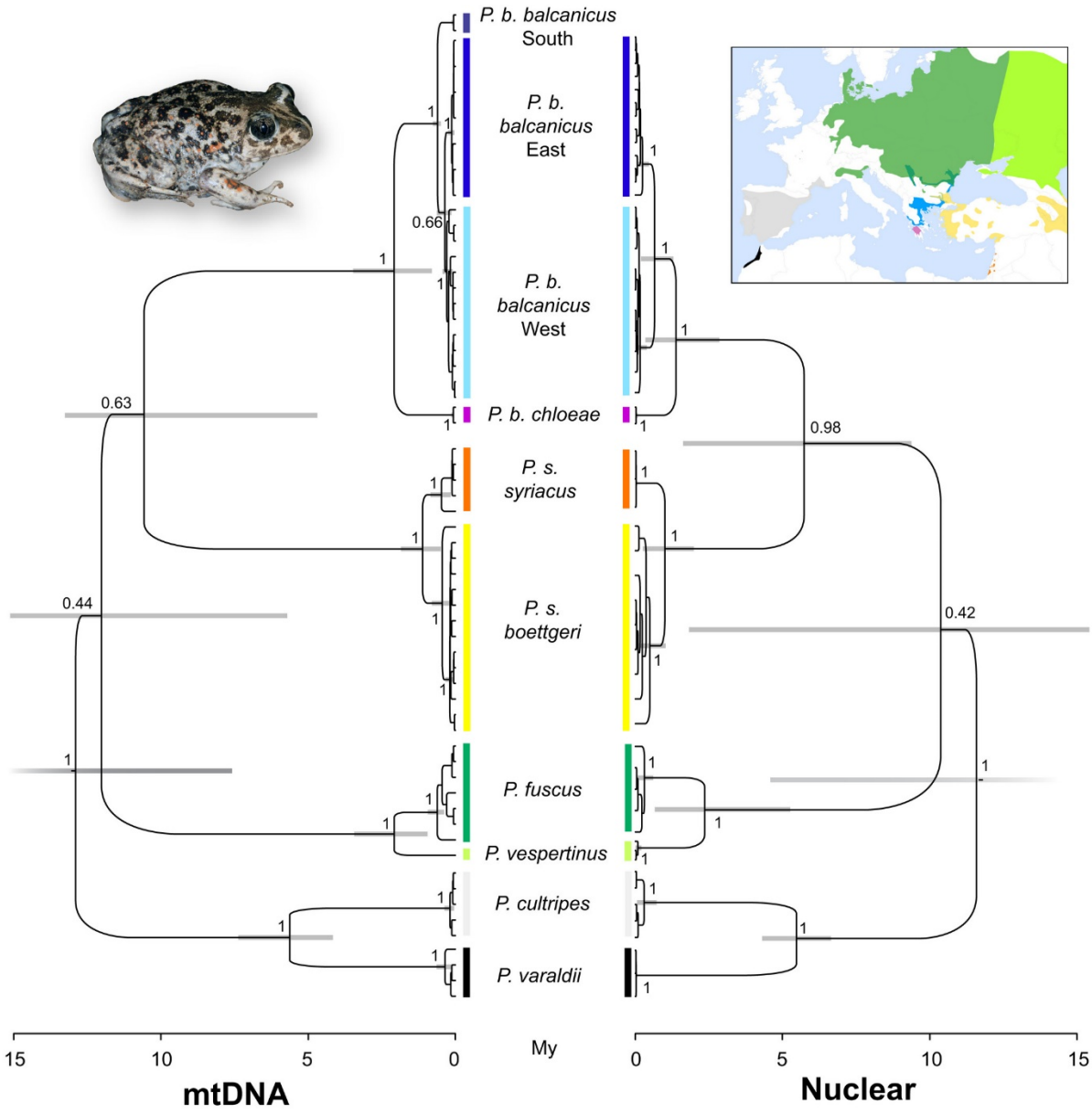

Figure 1 Time-calibrated phylogenetic relationships for Eurasian spadefoot toads (*Pelobates*) for mtDNA (*cyt-b* + 16S, 1.2 kb) and nuclear (538 RAD tags, 63.5 kb) sequences. Bayesian posterior probabilities are given for major nodes. Grey bars show the 95% confidence intervals of the divergence time estimates. Colours correspond to the maps provided in the other figures. Cloudograms are available in Figure S1. The map shows the distribution of all *Pelobates* taxa (Dufresnes et al., 2019). The top left picture illustrates the new Peloponnese subspecies *P. b. chloeae* discovered by this work (photo credit: C.D.)

The two axes of the PCA on 677 nuclear SNPs present in all species, cumulating 67.1% of the variance, also differentiated the six *Pelobates* species, grouped by sister taxa (Figure 2): *P. cultripes* with *P. varaldii*, *P. fuscus* with *P. vespertinus*, and *P. syriacus* with *P. balcanicus*.

3.2 Population genomics of *P. syriacus s.l*

Population genomic analyses support the intraspecific diversifications within *P. balcanicus* and *P. syriacus s.s*., and revealed the distribution of these lineages as well as gene flow between them. For *P. syriacus s.s*. (12,665 SNPs), the PCA primarily separates the Levantine *P. s. syriacus* (loc. 1–5) from *P. s. boettgeri* inhabiting the rest of the range (PC1, 25.2% of the variance; Figure 2). In the latter, Caucasus samples (loc. 6–9) stand out from the second axis (PC2, 15.0% of the variance; Figure 2). Analyses with structure (best for two and three groups, Figure S2) recovered the two subspecies (*P. s. syriacus* and *P. s. boettgeri*) and confirmed the distinctiveness of the Caucasian spadefoots (Figure 3). Several of these individuals, which had somewhat intermediate positions on the PCA, also showed intermediate ancestry coefficients, for example loc. 6–7. One *P. s. boettgeri* individual from loc. 17 (S-Turkey) possessed a *P. s. syriacus* mtDNA. Private mtDNA haplotypes were found in the Caucasus (loc. 7–9), although weakly differentiated from all others *P. s. boettgeri* (Figure S1).

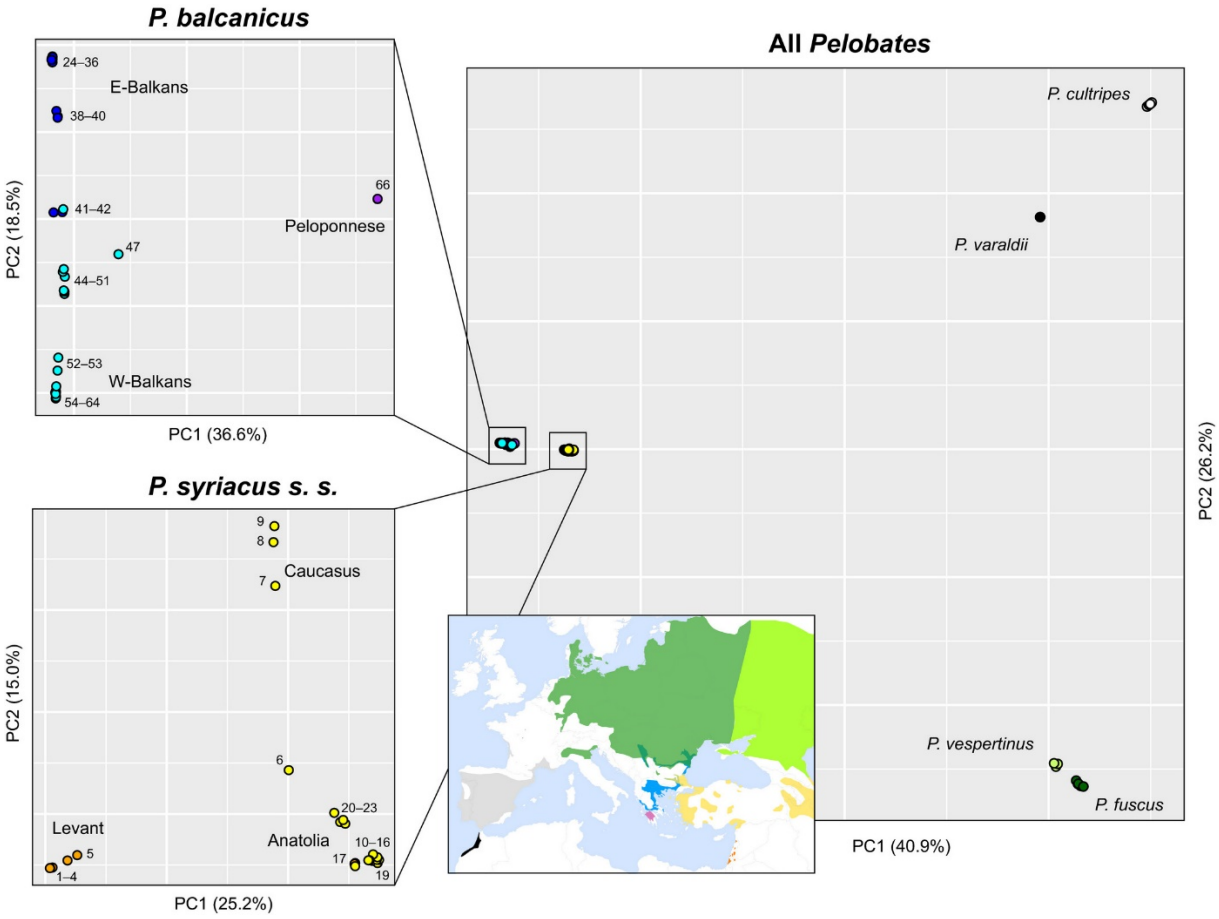

Figure 2 Principal component analysis (PCA) on nuclear SNPs for Eurasian spadefoot toads (*Pelobates*) (main frame, 677 SNPs), and within *P. balcanicus* (top left, 13,146 SNPs) and *P. syriacus s. s*. (bottom left, 12,665 SNPs). Dots are coloured according to mtDNA lineages. The map shows the distribution of all *Pelobates* taxa (Dufresnes et al., 2019). Note that the ranges of *P. vespertinus* and *P. s. boettgeri* extend further east

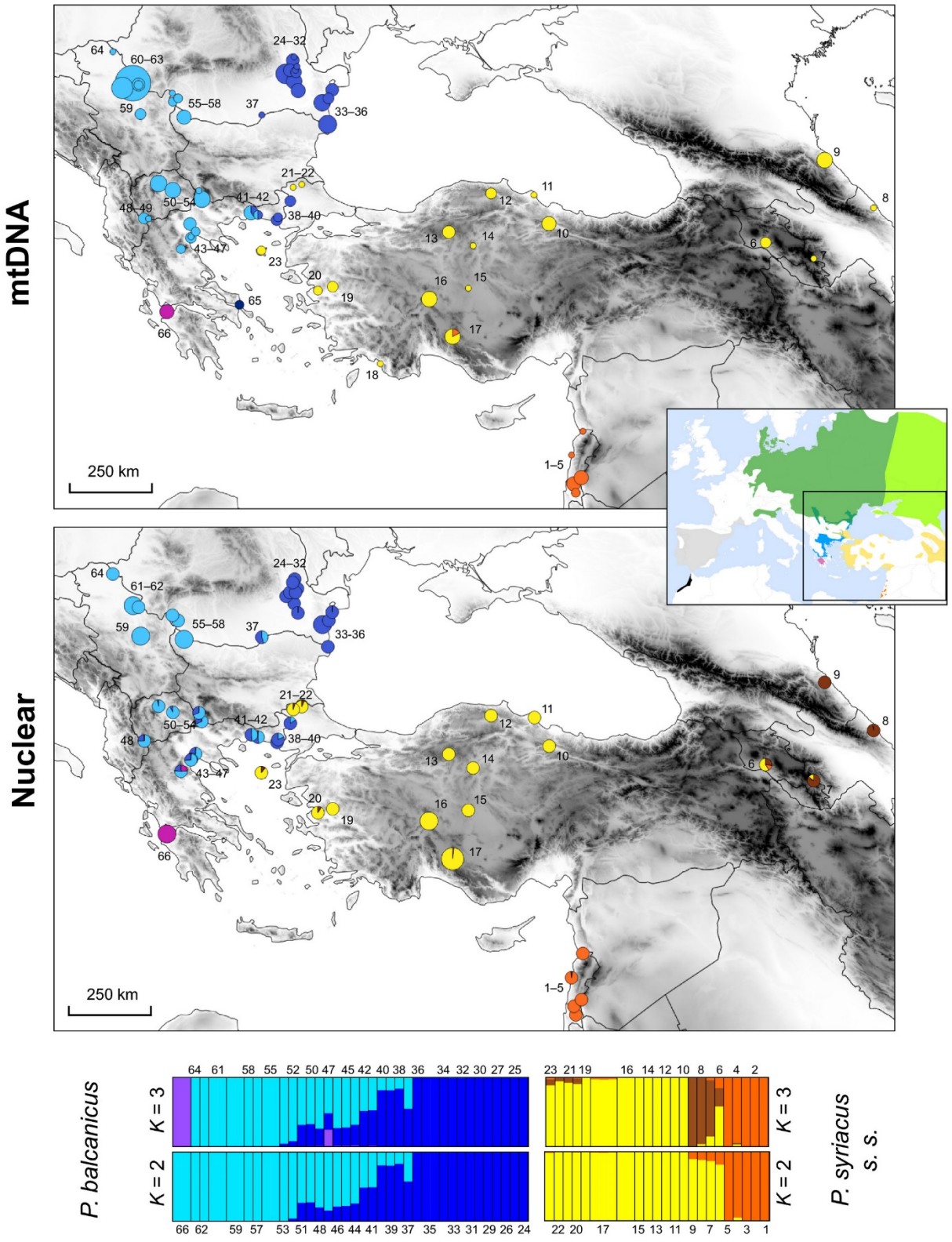

Figure 3 Phylogeography of *Pelobates balcanicus* (blue/purple) and *P. syriacus s.s.* (yellow/brown/orange). Top map: mtDNA distribution of the major lineages. Bottom map: nuclear distribution of the nuclear clusters inferred with structure ($K = 3$). Pie sizes are proportional to sample size. Analyses are based on 13,146 SNPs for *P. balcanicus* and 12,665 SNPs for *P. syriacus s.s.* The barplots show the structure ancestry coefficients of each individual for the $K = 2$ and $K = 3$ analyses, which best explain the data (Figure S2)

For *P. balcanicus* (13,146 SNPs), the PCA (Figure 2) and structure analyses with two and three groups (Figure 3, Figure S2) recovered the split of the Peloponnese *P. b. chloeae* sampled at loc. 66 (PC1, 36.6% of the variance), as well as the east–west differentiation across *P. b. balcanicus* from loc. 24–64 (PC2, 18.2% of the variance). Many populations of the latter taxon featured intermediate structure ancestry coefficients and intermediate position on PC2 (loc. 37–54), consistent with widespread admixture around the Carpathians and along the Danube. The mtDNA picture was largely concordant, but featured a narrower transition, with syntopy of the eastern and western *P. b. balcanicus* mitotypes in only two localities from NE-Greece (loc. 41 and 42). Moreover, the *P. b. balcanicus* loc. 47 sample showed admixture with *P. b. chloeae*. No RAD data are available to investigate the nuclear composition of the southern mtDNA subclade identified on Evia Island (loc. 65).

Demographic analyses of the widespread *P. b. balcanicus* and *P. s. boettgeri* yielded similar results (Figure S3): both lineages featured a 10-fold population expansion ~100,000 years ago, with no sign of population declines in their recent history. Genetic diversity was the highest for Western and Central Anatolian populations of *P. s. boettgeri*, as well as NE-Greece populations, where both lineages of *P. b. balcanicus* meet and admix (Figure S4). In contrast, the narrowly distributed *P. b. chloeae* had among the lowest levels of heterozygosity (Figure S4).

3.3 Analyses of *Pelobates* contact zones

Our intraspecific analyses revealed admixture between *P. s. syriacus* and *P. s. boettgeri*, between *P. b. chloeae* and *P. b. balcanicus*, as well as between the western and eastern *P. b. balcanicus* lineages (see 3.2). We further documented patterns of introgression across the contact zones of three different pairs of taxa (Figure 4). First, we did not detect gene flow between the sympatric *P. fuscus* and *P. b. balcanicus* in Serbia and Romania: all specimens of these two morphologically differentiated taxa possessed the corresponding mtDNA and were assigned to different nuclear clusters (Figure 4). Second, *P. b. balcanicus* and *P. s. boettgeri*, parapatric in European Turkey/NE-Greece, also show complete differentiation, except for a few samples with weak traces of nuclear admixture (<2%) near the area of contact (loc. 21–23, 38–40; Figure 4). Third, the *P. fuscus*/*vespertinus* hybrid zone in Ukraine and W-Russia involves admixed individuals across narrow transitions (loc. FV2–4, FV17–22; Figure 4). Mitochondrial and nuclear clines (analysed along FV16–24) were steep (nuclear cline width = 16.0 km, mtDNA cline width = 14.4 km) and concordant (nuclear cline centre = 131.7 km, mtDNA cline centre = 134.6 km) (Figure 5).

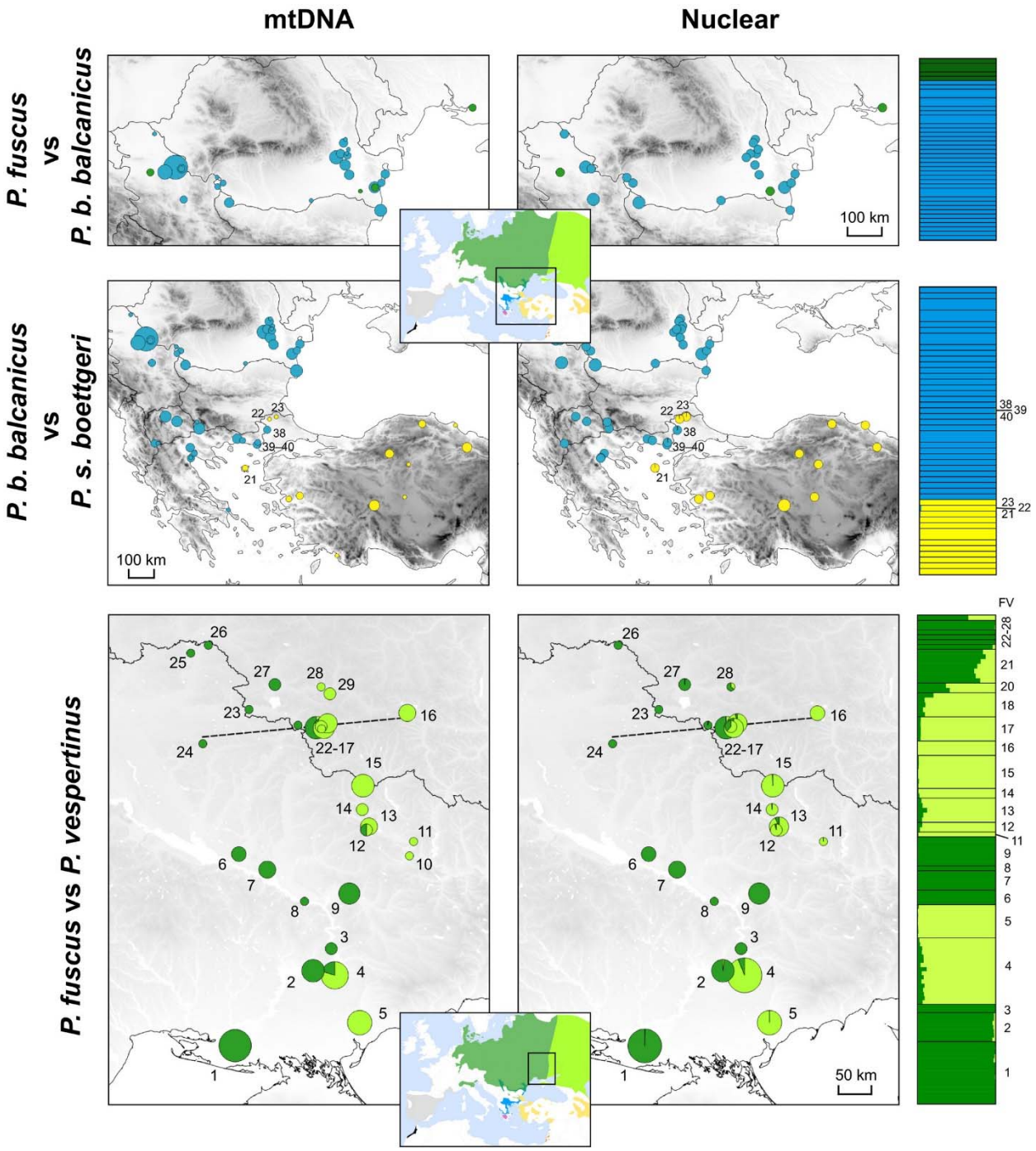

Figure 4 Population genomics of *Pelobates* contact zones in Eastern Europe. The left maps show mtDNA distributions and the right maps show nuclear distributions based on structure analyses ($K = 2$) of RAD data. Pie sizes are proportional to sample sizes. Top: *P. fuscus* (dark green, loc. detailed in Table S1) versus *P. b. balcanicus* (blue, loc. 24–64). Middle: *P. b. balcanicus* (blue, loc. 24–64) versus *P. s. boettgeri* (yellow, loc. 10–23). Bottom: *P. fuscus* (dark green) versus *P. vespertinus* (light green) across loc. FV1–28. Important localities are highlighted on the maps and structure barplots. The small framed maps show the distribution of all *Pelobates* taxa (Dufresnes et al., 2019)

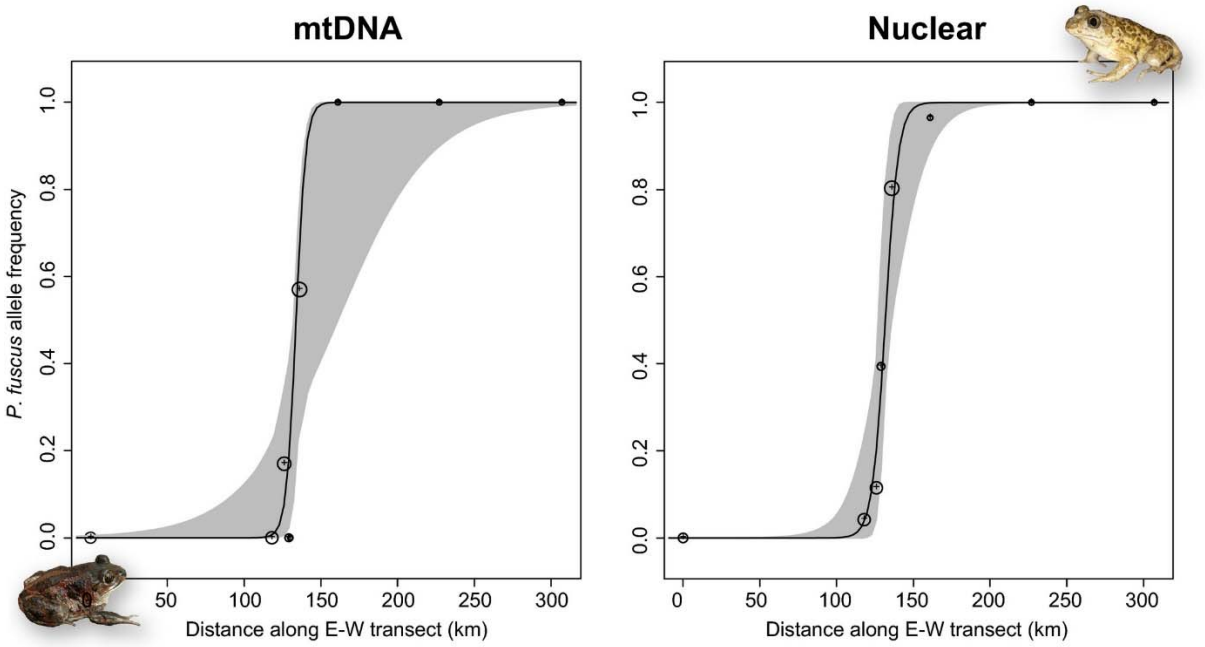

Figure 5 Cline analysis of the *P. fuscus*/*vespertinus* contact zone along an east–west transect (loc. FV16–24, see Figure 4). The best cline model involved only centre (*c*) and width (*w*) parameters, which were estimated to $c = 131.7$ and 134.6 for nuclear and mtDNA, respectively and $w = 16.0$ and 14.4 for nuclear and mtDNA, respectively (in km). Shaded areas represent 95% confidence intervals. Photo: *P. vespertinus* (left) by N. Su. and *P. fuscus* (right) by C.D.

4 DISCUSSION

Our study revealed that *Pelobates syriacus s.l.* is a superspecies that diversified from the Late Miocene to the Late Pleistocene, and features at least five cryptic lineages seemingly connected across four transition zones (Figure 3). Combined with our targeted analyses of the *P. fuscus*/*P. vespertinus* and *P. balcanicus*/*P. fuscus* contacts, this radiation thus provides an ad hoc framework to characterize the continuum of speciation along six different time points (Figure 6, Table 1), thus adding to a short list of comparative studies in lineage-rich cryptic radiations.

First, the mid-Miocene *P. fuscus* and *P. balcanicus* (>10 million years ago [My]) do not exchange genes despite sympatry and syntopy, confirming their complete reproductive isolation, probably involving premating barriers (Figure 4). It would be worthwhile to confirm this result by a replicate survey in the sympatric area of their respective sister taxa, *P. vespertinus* and *P. syriacus s.s.*, along the northwestern coast of the Caspian Sea (Mazanaeva & Askenderov, 2007).

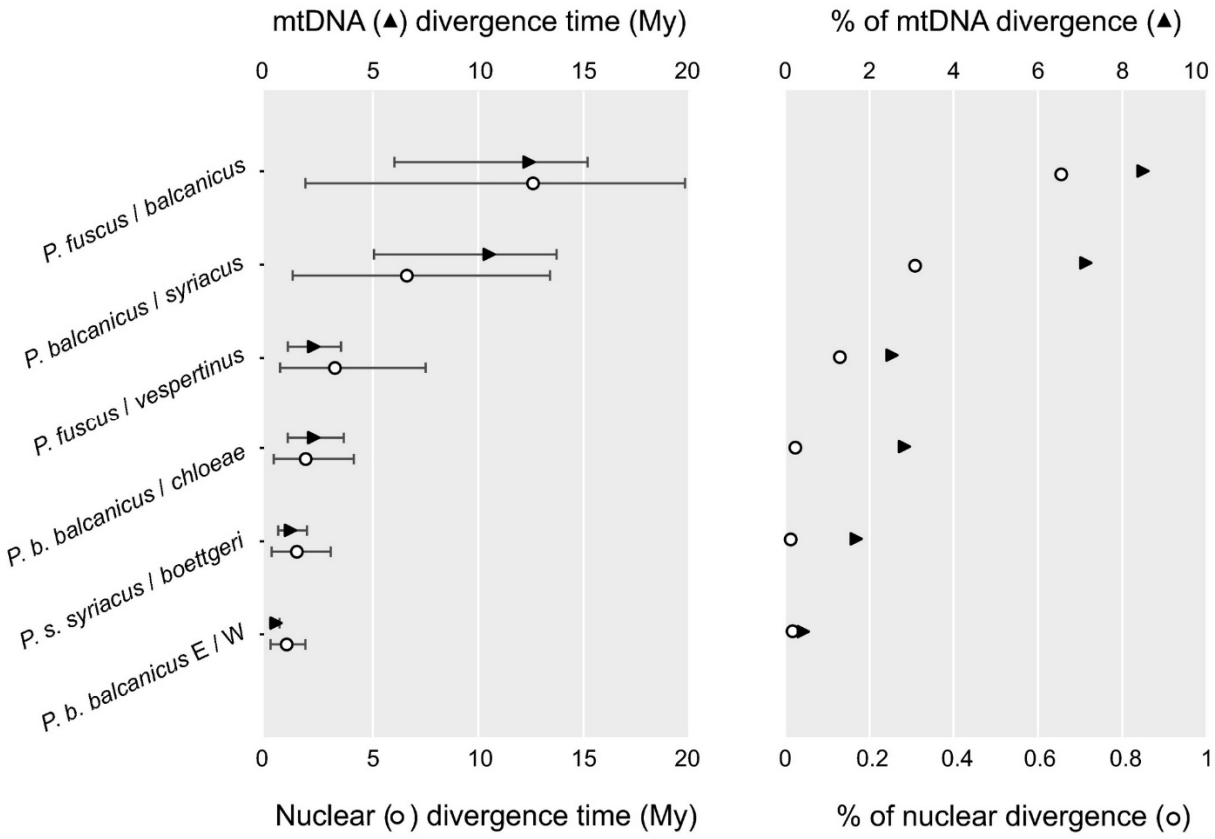

Figure 6 Estimated mitochondrial and nuclear divergence time (left) and sequence divergence (right) of six *Pelobates* pairs of taxa, arranged from the most admixing (bottom) to the least admixing (top); see Table 1. Using Spearman rank correlation tests, their respective hybridizability significantly relates to their divergence times and sequence divergence, for both mtDNA and nuclear estimates ($p < 0.05$). The tests remain significant when reshuffling the uncertain order of the two youngest pairs, which feature genetic introgression across hundreds of kilometres

Second, we characterized for the first time the lower Miocene taxa *P. balcanicus* and *P. syriacus s.s*., distributed in the Balkans and the Near-East, respectively (Figure 3). Their early split (5–10 My, Table 1, see also Veith et al., 2006 and Ehl et al., 2019) and very limited admixture (<2% among our parapatric samples) supports advanced if not complete reproductive isolation (Figure 4). These taxa thus merit a status as distinct species, as detailed in Dufresnes et al. (2019). Note that the unresolved internal nodes precluded accurate dating estimates, due to the uncertain position of the ancestor of *P. fuscus*/*vespertinus*. Nevertheless, our best-supported topologies, which group *P. syriacus s.s*. and *P. balcanicus* as sister clades (Figure 1, Figure S1), are consistent with morphological similarities (Dufresnes et al., 2019), as well as a previous mitochondrial phylogeny (Veith et al., 2006; with similar divergence time estimates). Future fine-scale sampling at their contact zone will be required to understand whether these form very localized hybrid zones, and if premating barriers evolved between these cryptic species.

Third, the Plio-Pleistocene *P. fuscus* and *P. vespertinus* (2–3 My, see also Veith et al., 2006; Crottini et al., 2007; Litvinchuk et al., 2013) admix in narrow transitions that we estimated to

be 14–16 km from our mtDNA and average nuclear cline analyses (Figures 4 and 5). From allozyme and genome size data (5% larger in *P. fuscus*, Suryadnaya, 2014), Litvinchuk et al. (2013) found quite similar cline estimates, namely 13 and 15 km, respectively. Under a tension zone model (Barton & Gale, 1993), and considering a conservative dispersal rate of about 1 km per generation (computed for smaller anuran amphibians; Szymura & Barton, 1991), a 15-km cline corresponds to a selective coefficient $s = 0.035$ at equilibrium, under intrinsic selection. Under a model of neutral diffusion, that is without any form of selection, the transitions would have exceeded 15 km in 36 generations since the initial contact. Assuming that *Pelobates* are sexually mature around 3 years (Oliveira, São-Pedro, Santos-Barrera, Penone, & Costa, 2017; Trochet et al., 2014) and can live up to 15 years (Cogălniceanu et al., 2014), 36 generations broadly represent 108–540 years. The contact between *P. vespertinus* and *P. fuscus* is clearly much older since their respective refugia, located on the western and eastern shores of the Black Sea (Crottini et al., 2007; Litvinchuk et al., 2013), are relatively close and connected by direct recolonization routes, without geographic barriers. There is thus little doubt that post-zygotic incompatibilities maintain the genetic integrity of *P. fuscus* and *P. vespertinus* despite hybridization in parapatric populations.

Fourth and fifth, the Pleistocene clades discovered within *P. balcanicus* (~2 My) and *P. syriacus s. s*. (~1 My), that we consider as subspecies (Dufresnes et al., 2019), potentially admix over wide areas, indicative of little or no hybrid incompatibility. In the Balkans, hybridization was detected in one locality between *P. b. balcanicus* and *P. b. chloeae* (loc. 47, Figure 3) but a large sampling gap remains over Central Greece. In *P. syriacus s.s*., traces of nuclear and mtDNA of the Levantine subspecies (*P. s. syriacus*) are found in Anatolia and the Caucasus (*P. s. boettgeri*), that is over hundreds of kilometres apart, despite current population fragmentation. Caucasian spadefoots might actually have a mixed origin, given their introgressed ancestry (Figure 3).

Sixth, the shallow phylogeographic lineages of *P. b. balcanicus* (<1 My) merged over hundreds of kilometers (Figure 3), characteristic of lineage fusion (Garrick, Banusiewicz, Burgess, Hyseni, & Symula, 2019). These probably represent ephemeral divergences generated by glacial isolation, which are commonplace in the Balkans (e.g., Dufresnes et al., 2013). Projected species distribution models accordingly flagged suitable conditions around the Carpathians during the Last Glacial Maximum (Iosif et al., 2014). As supported by the demographic reconstruction (Figure S3), we hypothesize that these lineages expanded from separate eastern (Black Sea coast) and western (Pannonian Basin) refugia, resulting in the widespread admixture (and inflated heterozygosity) observed along the Danube and the northeastern Greek Coast.

Patterns of introgression in *Pelobates* thus bring new empirical support that cryptic phylogeographic splits of increasing depth represent different stages along the speciation continuum, from evolutionary ephemera to nascent species (Figure 6, Table 1). Our results mirror the pioneer findings of Singhal and Moritz (2013), who quantified an increase of reproductive isolation among Australian skink hybrid zones, in respect to their relative ages. Rather than linear, this study reported an exponential buildup of reproductive isolation, implying that barriers to gene flow can grow quickly once they are initiated, as accumulating

DMIs multiply their effects. Given our unequal sampling for several contacts, here we established a qualitative, statistically supported link across the gradient of differentiation (Figure 6, Table 1), but could not assess the shape of the relationship. Nevertheless, from our data, the "grey zone of speciation" (i.e. the window of divergence across which nascent species do not merge, but still frequently hybridize) is remarkably narrow (Roux et al., 2016): <1 million years separates the admixing subspecies *P. b. balcanicus*/*chloeae* (pending proper analyses of their hybrid zone) from the nearly impermeable genomes of *P. fuscus* and *P. vespertinus*. In contrast, the alternative situation where barriers to gene flow emerge suddenly, due to few genes or gene complexes (e.g., supergenes) with major effects (Servedio, van Doorn, Kopp, Frame, & Nosil, 2011), better applies to systems where ecological and behavioural divergence is a major driver of reproductive isolation (e.g., Jay et al., 2018), not to ecomorphologically cryptic species diverging in allopatry.

Given the lack of phenotypic and environmental differentiation among all *Pelobates* pairs tested except one (the oldest split, *P. balcanicus*/*P. fuscus*; but see Iosif et al., 2014), and although we cannot rule out some cryptic premating or local adaptation mechanisms, reproductive isolation should be essentially intrinsic and thus mostly dependent on the amount of divergence accumulated during the time spent in allopatry. As such, the age of the split between *P. fuscus* and *P. vespertinus* (~3 My from the RAD data), which show advanced (but not complete) reproductive isolation, can serve as a benchmark for the tempo of allopatric speciation in these toads. In other cryptic amphibian radiations, unimodal yet narrow transitions (<50 km) span from a similar age (2–3 My) in *Pelodytes* (Díaz-Rodríguez et al., 2017) and *Bufotes* (Dufresnes et al., 2014), to divergence times twice as old, for example 5 My in *Hyla* (Dufresnes et al., 2015), and 4–7 My in *Triturus* (Arntzen et al., 2014; Wielstra, McCartney-Meslstad, Arntzen, Butlin, & Shaffer, 2019). Beyond methodological differences such as sampling design, type of molecular markers, and calibration settings of molecular clocks, this overall variation also reflects stochastic effects on local hybrid zone dynamics (e.g., dispersal opportunities, local demographic events), which confound reproductive isolation. In addition, patterns of admixture can drastically differ between replicate hybrid zones of the same species pairs, depending on the intraspecific lineages involved (e.g., Arntzen, de Vries, Canestrelli, & Martínez-Solano, 2017), emphasizing how the random nature of DMI accumulation can increase variance in the timeline of reproductive isolation. Finally, divergent selection on ecomorphology may skew the rate to which reproductive isolation accumulates among lineages (Gavrilets, 2004). This may typically affect the *Triturus* model, where "cryptic" species evolve towards differing lifestyles (Arntzen, 2003; Wielstra et al., 2019) and feature hybrid zones moving along environmental gradients (Arntzen & Wallis, 1991).

While the continuous nature of speciation is one of the best accepted concepts in evolutionary biology (Mallet, 1995), the literature on cryptic speciation mainly consists of a collection of independent case studies and very few allow to grasp this continuum among a single phylogenetic group. Our data on *Pelobates* thus add to a growing body of evidence that reproductive isolation is mostly a gradual, dynamic, yet reversible process (e.g., Seehausen, 2006; Hendry, Bolnick, Berner, & Peichel, 2009), at least during the initial stages of divergence. This is well exemplified here by the evanescent lineages of *P. b. balcanicus*, now merging back

following post-glacial secondary contact. *Pelobates s. syriacus* and *P. s. boettgeri* would probably face the same fate if their ranges were not recurrently fragmented, and instead these lineages will most likely continue to diverge. Because they still experience episodic gene flow, their leaky boundaries may be a vector of diversity, here contributing to the mixed genetic nature of the Caucasian populations. As cryptic diversifications offer windows on the evolutionary spectrum from population divergence to speciation, without the confounding effects of extrinsic factors, they hold great potential for our understanding of the genetic basis of species formation in space and time, now more than ever in the genomic era.

ACKNOWLEDGEMENTS

We are grateful to L. J. Borkin, E. Bozkurt, D. Donaire, G. Džukić, V. Fradet, M. Kalezić, G. A. Lada, L. F. Mazanaeva, K. D. Milto, V. F. Orlova, J. Secondi, D. A. Shabanov, D. V. Skorinov, F. Stănescu, D. Székely, A. Teynié, E. Tzoras and O. Zinenko, who greatly contributed during fieldtrips or provided tissue samples. We also thank the Genomic Technologies Facility (GTF) of the University of Lausanne. American outgroup samples were kindly shared by the Fujita lab from the University of Texas (Arlington, TX, USA; via Jose Maldonado). We are grateful to E. Twomey, along with two anonymous reviewers for their useful comments. Fieldwork in Romania was supported by a Romanian National Authority for Scientific Research grant, CNCS-UEFISCDI, project number PN-II-ID-PCE-2011-3-0173 to D.C. This research was supported by a bilateral grant from Wallonie-Bruxelles International and CCCDI-UEFISCDI (ANCS) to M.D. and D.C. (no. 105BM), a grant from the Serbian Ministry of Education, Science and Technological Development (project no. 173043) to T.V., a grant from the Swiss National Science Foundation (SNSF) to N.P. (no. 31003A_166323), and an SNSF fellowship to C.D. (no. P2LAP3_171818). M.D. is Research Director at Fonds de la Recherche scientifique – FNRS.

AUTHOR CONTRIBUTIONS

C.D., S.N.L. and M.D. designed the study. All authors performed sampling. C.D. conducted the labwork, analyses and drafted the paper, which was subsequently improved by all co-authors.

DATA AVAILABILITY STATEMENT

The data supporting this study are openly available on GenBank under accessions MK902544–MK902597 (*cyt-b* haplotypes) and MK902523–MK902543 (16S haplotypes), as well as on the NCBI sequence read archive (SRA; Dufresnes, 2019) under BioProject PRJNA542138 with accessions SAMN11612144–SAMN11612336 (raw individual RAD sequences).

REFERENCES

Arntzen, J. W., Wielstra, B., & Wallis, G. P. (2014). The modality of nine *Triturus* newt hybrid zones assessed with nuclear, mitochondrial and morphological data. *Biological Journal of the Linnean Society, 113*, 604-622.

Arntzen, J. W., de Vries, W., Canestrelli, D., & Martinez-Solano, I. (2017) Hybrid zone formation and contrasting outcomes of secondary contact over transects in common toads. *Molecular Ecology, 26*, 5663-5675.

Avise, J., Walker, D., & Johns, G. (1998). Speciation durations and Pleistocene effects on vertebrate phylogeography. *Proceedings of the Royal Society B: Biological Sciences, 265,* 1707–1712.

Avise, J. (2000). Phylogeography: The history and formation of species. Cambridge, MA, Harvard University Press.

Barton, N. H., & Hewitt, G. M. (1985) Analysis of hybrid zones. *Annual Review of Ecology and Systematics, 16*, 113–148.

Barton, N., & Gale, K. S. (1993). Genetic analysis of hybrid zones. In: R. Harrison (Ed), *Hybrid zones and the evolutionary process* (pp. 13-45). New York City (NY): Oxford Universit Press.

Beysard, N., & Heckel, G. (2014). Structure and dynamics of hybrid zones at different stages of speciation in the common vole (*Microtus arvalis*). *Molecular Ecology, 23*, 673-687.

Bickford, D., Lohman, D., Sodhi, N., Ng, P., Meier, R., Winker, K., …Das, I. (2006). Cryptic species as a window on diversity and conservation. *Trends in Ecology & Evolution, 22*, 148–155.

Borkin, L. J., Litvinchuk, S. N., Rosanov, M., Khalturin, M. D., Lada, G. A., Borissovsky, A. G., … Ruchin, A. (2003). New data on the distribution of two cryptic forms of the common spadefoot toads (*Pelobates fuscus*) in eastern Europe. *Russian Journal of Herpetology, 10*, 115-122.

Bouckaert, R. R., & Heled, J. (2014). DensiTree 2: seeing trees through the forest. Retrieved from http://dx.doi.org/10.1101/012401.

Bouckaert, R., Heled, K., Khünert, D., Vaughan, T., Wu, C. H., Xie ,D., … Drummond, A. J. (2014). BEAST 2: A software platform for Bayesian Evolutionary Analysis. *PLoS Computational Biology, 10*, e1003537.

Bouckaert, R. R., & Drummond, A. J. (2017). bModelTest: Bayesian phylogenetic site model averaging and model comparison. *BMC Evolutionary Biology, 17*, 42.

Brelsford, A., Dufresnes, C., & Perrin, N. (2016a). High-density sex-specific linkage maps of a European tree frog (*Hyla arborea*) identify the sex chromosome without information on offspring sex. *Heredity, 116*, 177-181.

Catchen, J., Hohenlohe, P., Bassham, S., Amores, A., & Cresko, W. (2013). Stacks: an analysis tool set for population genomics. *Molecular Ecology, 22*, 3124-3140.

Coates, D. J., Byrne, M., & Moritz, C. (2018). Genetic diversity and conservation units: dealing with the speciation-population continuum in the age of genomics. *Frontiers in Ecology & Evolution, 6*, 165.

Crottini, A., Andreone, F., Kosuch, J., Borkin, L., Litvinchuk, S. N., Eggert, C., & Veith, M. (2007). Fossorial but widespread: the phylogeography of the common spadefoot toad (*Pelobates fuscus*), and the role of the Po Valley as a major source of genetic variability. *Molecular Ecology, 16*, 2734-2754.

Croucher, P. J., Jones, R. M., Searle, J. B., & Oxford, G. S. (2007). Contrasting patterns of hybridization in large house spiders (*Tegenaria atrica* group, Agelenidae). *Evolution, 61*, 1622-1640.

Derryberry, E. P., Derryberry, G. E., Maley, J. M., & Brumfield R,T. (2014). HZAR: hybrid zone analysis using an R software package. *Molecular Ecology Resources, 14*, 652-663.

Diaz-Rodriguez, J., Gehara, M., Marquez, R., Vences, M., Goncalves, H., Sequeira, F., … Tejedo, M. (2017). Integration of molecular, bioacoustical and morphological data reveals two new cryptic species of *Pelodytes* (Anura, Pelodytidae) from the Iberian Peninsula. *Zootaxa, 4243*, 1-41.

Dufresnes, C., Bonato, L., Novarini, N., Betto-Colliard, C., Perrin, N., & Stöck, M. (2014). Inferring the degree of incipient speciation in secondary contact zones of closely related lineages of Palearctic green toads (*Bufo viridis* subgroup). *Heredity, 113*, 9-20.

Dufresnes, C., Brelsford, A., Crnobrnja-Isailovic, J., Tzankov, N., Lymberakis, P., & Perrin, N. (2015). Timeframe of speciation inferred from secondary contact zones in the European tree frog radiation (*Hyla arborea* group). *BMC Evolutionary Biology, 15*, 155.

Dufresnes, C., Mazepa, G., Rodrigues, N., Brelsford, A., Litvinchuk, S. N, Sermier, R., … Jeffries, D. L. (2018). Genomic evidence for cryptic speciation in tree frogs from the Apennine Peninsula, with description of *Hyla perrini* sp. nov. *Frontiers in Ecology & Evolution 6,* 144.

Dufresnes, C., Strachinis, I., Tzoras, E., Litvinchuk, S., & Denoël M. Call a spade a spade: taxonomy and distribution of *Pelobates*, with description of a new Balkan endemic. *Zookeys*, in review.

Dufresnes, C. (2019). Amphibians of Europe, North Africa and the Middle East. London, United Kingdom: Bloomsbury eds.

Earl, D. A., & vonHoldt, B. M. (2012). STRUCTURE HARVESTER: a website and program for visualizing STRUCTURE output and implementing the Evanno method. *Conservation Genetics Resources, 4,* 359-361.

Ehl, S., Vences, M., & Veith, M. (2019). Reconstructing evolution at the community level: a case study on Mediterranean amphibians. *Molecular Phylogenetics & Evolution, 134*, 211-225.

Heled, J., Drummond, A. J. (2008). Bayesian inference of population size history from multiple loci. *BMC Evolutionary Biology, 8*, 289.

Heled, J. (2010). Extended Bayesian Skyline Plots tutorial. Retrieved from: tutorial.east.bio.ed.ac.uk/Tutorials.

Heled, J. (2015). Extended Bayesian Skyline Plot tutorial for BEAST 2. Retrieved from: http://evomicsorg.wpengine.netdna-cdn.com/wp-content/uploads/2015/11/ebsp2-tut1.pdf

Hendry, A. P., Bolnick, D. I., Berner, D., & Peichel, C. L. (2009). Along the speciation continuum in sticklebacks. *Journal of Fish Biology, 75*, 2000-2036.

Garcia-Paris, M., Buchholz, D. R., & Parra-Olea, G. (2003). Phylogenetic relationships of Pelobatidae re-examined using mtDNA. *Molecular Phylogenetics and Evolution, 28*, 12-23.

Gavrilets, S. (2004). Fitness landscapes and the origin of species. Cambridge, MA: Princeton University Press.

Gourbiere, S., & Mallet, J. (2009). Are species real? The shape of the species boundary with exponential failure, reinforcement and the 'missing snowball'. *Evolution, 64*, 1–24

Iosif, R., Papes, M., Samoila, C., & Cogălniceanu, D. (2014). Climate-induced shifts in the niche similarity of two related spadefoot toads (genus *Pelobates*). *Organisms Diversity & Evolution, 14*, 397-408.

Jay, P, Whibley, A, Frézal, L, Rodriguez de Cara, M. A., Nowell, R. W., Mallet, J, … Joron, M. (2018). Supergene evolution triggered by the introgression of a chromosomal inversion. *Current Biology, 28*, 1-7.

Jombart, T. (2008). adegenet: a R package for the multivariate analysis of genetic markers. *Bioinformatics, 24*, 1403-1405.

Litvinchuk, S. N., Crottini, A., Federici, S., De Pous, P., Donaire, D., Andreone, F., ... Rosanov, J. M. (2013). Phylogeographic patterns of genetic diversity in the common spadefoot toad, *Pelobates fuscus* (Anura: Pelobatidae), reveals evolutionary history, postglacial range expansion and secondary contact. *Organisms Diversity & Evolution 13*, 433-451.

Mallet, J. (1995). A species definition for the modern synthesis. *Trends in Ecology & Evolution, 10*, 294–299.

Mazanaeva, L. F., & Askenderov, A. D. (2007). New data on the distribution of eastern spadefoot, *Pelobates syriacus* Boettger, 1889, and common spadefoot, *Pelobates fuscus*, Laurenti, 1768, in Dagestan (the North Caucasus). *Russian Journal of Herpetology, 14*, 161-166.

Mendelson, T., Inouye, B., & Rausher, M. (2004). Quantifying patterns in the evolution of reproductive isolation. *Evolution, 58*, 1424–1433.

Mérot, C., Salazar, C., Merrill, R. M., Jiggins, C. D., & Joron, M. (2017). What shapes the speciation continuum of reproductive isolation? Lessons from *Heliconius* butterflies. *Proceedings of the Royal Society B: Biological Sciences, 284*, 20170335.

Morgan-Richards, M., & Wallis, G. (2003) A comparison of five hybrid zones of the weta *Hemideina thoracica* (Orthoptera: Anostomatidae): degree of cytogenetic differentiation fails to predict zone width. *Evolution, 57*, 849-861.

Nosil, P., Feder, J., Flaxman, S. M., & Gompert. Z. (2017). Tipping points in the dynamics of speciation. *Nature Ecology and Evolution* 1: 0001.

Oliveira, B. F., São-Pedro, V. A., Santos-Barrera, G., Penone, C., & Costa, G. C. (2017). AmphiBIO, a global database for amphibian ecological traits. *Scientific Data, 4,* 170123.

Orr, H. (1995). The population genetics of speciation: the evolution of hybrid incompatibilities. *Genetics, 139*, 1805–1813.

Pabijan, M., Zielinski, P., Dudek, K., Stuglik, M., & Babik, W. (2017). Isolation and gene flow in a speciation continuum in newts. *Molecular Phylogenetic & Evolution, 116*, 1-12.

Padial, J., Miralles, A., De la Riva, I., & Vences, M. (2010). The integrative future of taxonomy. *Frontiers in Zoology, 7*, 16.

Pritchard, J. K, Stephens, M., & Donnelly, P. (2000). Inference of population structure using multilocus genotype data. *Genetics, 155*, 945–959.

Roux, C, Fraïsse, C., Romiguier, J., Anciaux, Y., Galtier, N., & Bierne, N. (2016). Shedding light on the grey zone of speciation along a continuum of genomic divergence. *PLoS Biology, 14*, e20000234.

Seehausen, O. (2006) Conservation: losing biodiversity by reverse speciation. *Current Biology, 16*, 334–347.

Servedio, M. R., van Doorn, G. S., Kopp, M., Frame, A. M., & Nosil, P. (2011). Magic traits in speciation: "magic" but not rare? *Trends in Ecology & Evolution, 26*, 389-397.

Singhal, S., & Moritz, C. (2013). Reproductive isolation between phylogeographic lineages scales with divergence. *Proceedings of the Royal Society B: Biological Sciences, 280*, 20132246.

Smadja, C. M., Butlin, R. K. (2011). A framework for comparing processes of speciation in the presence of gene flow. *Molecular Ecology, 20*, 5123–5140.

Stöck, M., Dufresnes, C., Litvinchuk, S. N., Lymberakis, P., Biollay, S., Berroneau, M., … Perrin, N. (2012). Cryptic diversity among Western Palearctic tree frogs: postglacial range expansions, range limits, and secondary contacts of three European tree frog lineages (*Hyla arborea* group). *Molecular Phylogenetics & Evolution, 65*, 1-9.

Stoffel, C., Dufresnes, C., Okello, J. B., Noirard, C., Joly, P., Nyakaana, S., …Fumagalli, L. (2015). Genetic consequences of population expansions and contractions in the common hippopotamus (*Hippopotamus amphibius*) since the Late Pleistocene. *Molecular Ecology, 24*, 2507-2520.

Suryadnaya, N. N. (2014). Comparative analysis of karyotypes of two cryptic species of pelobatid frogs (Amphibia, Anura) of Ukraine. *Vestnik zoologii, 48*, 511-520.

Suriadna, N. N., Mikitinets, G. I., Rozanov Yu, M., Litvinchuk, S. N. (2016). Distribution, morphological variability and peculiarities of biology of spadefoot toads (Amphibia, Anura, Pelobatidae) in the south of Ukraine. *Proceedings of the Zoological Museum of Kiïv, 47*, 80-87.

Szymura, J. M., & Barton, N. H. (1991). The genetic structure of the hybrid zone between the fire-bellied toads *Bombina bombina* and *B. variegata*: comparisons between transects and between loci. *Evolution, 45*, 237-261.

Trochet, A., Moulherat, S., Calvez, O., Stevens, V. M., Clobert, J., & Schmeller, D. S. (2014). A database of life-history traits of European amphibians. *Biodiversity Data Journal, 2*, e4123.

Veith, M., Fromhage, L., Kosuch, J., Vences, M. (2006). Historical biogeography of Western Palaearctic pelobatid and pelodytid frogs: a molecular phylogenetic perspective. *Contribution to Zoology, 75*, 109-120.

Wielstra, B., Burke, T., Butlin, R. K., Avci, A., Uzüm, N., Bozkurt, E., … Arntzen, J. W. (2017a). A genomic footprint of hybrid zone movement in crested newts. *Evolution Letters, 1*, 93-101.

Wielstra, B., Burke, T., Butlin, R. K., & Arntzen, J. W. (2017b). A signature of dynamic biogeography: enclaves indicate past species replacement. *Proceedings of the Royal Society B, Biological Sciences, 284*, 20172014.

Wielstra, B., McCartney-Meslstad, E., Arntzen, J. W., Butlin, R. K., & Shaffer, H. B. (2019). Phylogenomics of the adaptive radiation of *Triturus* newts supports gradual ecological niche expansion towards an incrementally aquatic lifestyle. *Molecular Phylogenetics & Evolution, 133*, 120-127.